



Research Article

ISSN : 0975-7384
CODEN(USA) : JCPRC5

Effects of doping Ni^{2+} on the structure and photocatalytic denitrification activity of Bi_2WO_6 f Bi

Yan Huagao and Ying Chen

Provincial Key Laboratory of Oil and Gas Chemical Technology, College of Chemistry and Chemical Engineering, Northeast Petroleum University, Daqing, Heilongjiang, China

ABSTRACT

The Ni-doped Bismuth tungstate (Bi_2WO_6) microcrystalline was successfully prepared by a facile hydrothermal route. The samples were characterized by XRD, SEM, UV-vis, EDS, BTE and Py-FT-IR. The photocatalytic denitrification performance of Ni/ Bi_2WO_6 catalysts was measured by photocatalytic denitrification of simulation oil containing nitrogenous adopted as the model compound. The results showed that the structure of the catalyst changed by doping with Ni. More stable three-dimensional nanoparticles were found causing compact structure. The scope of the visible spectrum was expanded because of changing of energy gap from 2.67eV to 2.57eV and the photocatalytic activity was improved. The photocatalytic denitrification rate of the Ni/ Bi_2WO_6 powder could reach to 94% under the xenon lamp light irradiation with the following conditions that photocatalytic reaction time was 120 min, 1% Ni^{2+} doped, and the ratio of catalyst and oil was 2 mg/40ml.

Key words: Ni-doped, Bi_2WO_6 , photocatalysis, denitrification

INTRODUCTION

The nitrogen content of crude oil product is generally much higher which is 0.1%~0.5% in China. The content of nitrides in the fuel oil is restricted strictly with the increasing environmental awareness. The nitrides in the fuel oil, especially the basic nitrogen compounds are bad for the stability, performance and subsequent catalytic processing.^{1,2} So it is very important to produce clean oil. Recently, photocatalytic denitrification as a new oil denitrification technology attracted more attention, and it is very practical for enhancing the stability of light oil.

Bi_2WO_6 is a new kind of semiconductor photocatalytic material with high stability, high efficiency and environmental property which is belonged to Aurivillius oxides and having three-dimensional layered structure.³ The layer structure could help the photon-accomplishd carriers to drift and improve the quatum effieciency of the photocatalysts.⁴ In recent years, Bi_2WO_6 was wildely used on degradation of methylthionine chloride, rhodamine, 4-chlorine phenol etc. in waste water, and the applications on the denitrification of light oil.⁵⁻⁷ In this paper the $\text{Ni}^{2+}/\text{Bi}_2\text{WO}_6$ photocatalyst with high activity was prepared firstly, then the factors influencing the appearance of the catalyst and the denitrification activity were studied.

EXPERIMENTAL SECTION

2.1 Materials

$\text{Bi}(\text{NO}_3)_3 \cdot 5\text{H}_2\text{O}$ was purchased from Beijing Chemical Plant, CTAB was purchased from Shanghai Chemical Reagent Co.,Ltd., $\text{Na}_2\text{WO}_4 \cdot 2\text{H}_2\text{O}$, absolute ethyl alcohol and $\text{Ni}(\text{NO}_3)_2 \cdot 6\text{H}_2\text{O}$ were purchased from Tianjin Kemiou Chemical Reagent Co.,Ltd.. All chemicals were analytical grade.

2.2 Preparation of the catalyst

In a typical process, 0.971g of $\text{Bi}(\text{NO}_3)_3 \cdot 5\text{H}_2\text{O}$ was dissolved in 10 mL nitric acid solution and 0.329g of $\text{NaWO}_4 \cdot 2\text{H}_2\text{O}$ was dissolved in 20 mL of deionized water that were in ultrasound for 5min respectively. Then, the $\text{NaWO}_4 \cdot 2\text{H}_2\text{O}$ solution was added into the $\text{Bi}(\text{NO}_3)_3 \cdot 5\text{H}_2\text{O}$ solution dropwise. After reacted with each other sufficiently, the $\text{Ni}(\text{NO}_3)_2 \cdot 6\text{H}_2\text{O}$ was added into the above reaction product and stirred for 30 min and then be heated to 180 °C for 24h. The product was cooled to room temperature and filtered, washed with absolute ethyl alcohol and deionized water for several times until pH value was close to 7, dried at 80°C for 80h in air and the catalyst was prepared at last.

2.3 Characterization

The crystalline structure of the catalyst was characterized by powder X-ray (XRD, DMAX-2000) and X-ray energy dispersive spectrometer (Oxford InCa). Fourier transforms infrared (FTIR) spectra were collected on KBr-diluted pelletized samples using a Bruker Optics Tensor-27 spectrophotometer. The constitution of the catalyst was observed by The morphology of the catalyst was observed on a scanning electron microscope (SEM, EVOMA25). The UV-vis spectrum of the catalyst was measured on a UV-vis spectrophotometer (UV-759). The specific surface area of the catalyst was calculated by the Brunauer-Emmett-Teller method (BET, NOVA-2000E).

2.4 Catalytic test

The photocatalytic activity of $\text{Ni}^{2+}/\text{Bi}_2\text{WO}_6$ was evaluated by the denitrification degree of simulated oil mainly containing pyridine in light petroleum. In a typical operation, the catalyst, simulated oil and stirrer were added into the reactor which was shined by a 500-W xenon lamp and the ratio of catalyst to oil was 20 mg/40ml . The nitrogen content in the simulated oil was determined by the method for measuring basic nitrogen content in petroleum products (SH-T01629)^[8].

RESULTS AND DISCUSSION

3.1 Characterization of the $\text{Ni}^{2+}/\text{Bi}_2\text{WO}_6$ catalyst

3.1.1 XRD patterns of the $\text{Ni}^{2+}/\text{Bi}_2\text{WO}_6$

The XRD patterns of the $\text{Ni}^{2+}/\text{Bi}_2\text{WO}_6$ catalysts with different Ni^{2+} were shown in Figure 1. The diffraction peaks could be easily indexed to be orthorhombic that were typical for Bi_2WO_6 (JCPDS No. 39-0256). After doping the position of the typical peaks were not changed but only more intense indicating that all the samples are pure Bi_2WO_6 .

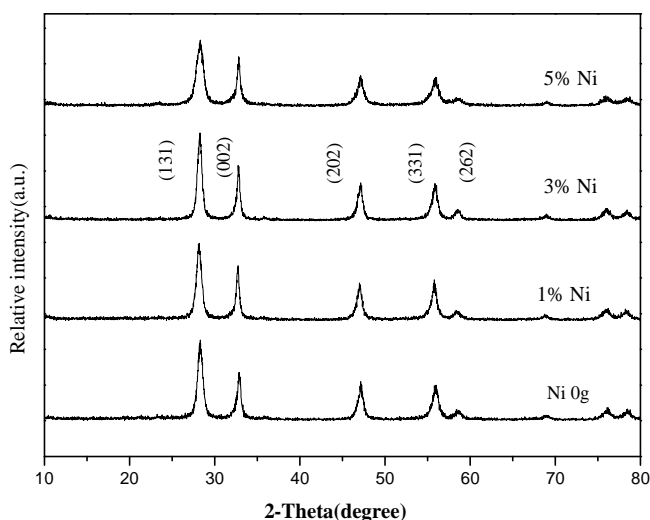


Fig. 1 XRD patterns of Bi_2WO_6 with various Ni loading

3.1.2 EDS Analysis of $\text{Ni}^{2+}/\text{Bi}_2\text{WO}_6$

Figure 2 showed the EDS images of the Bi_2WO_6 with different Ni^{2+} . It could be found that Bi_2WO_6 was consisted of Bi, W, O and Ni, indicating high purity. The ratio of Bi:W:O:Ni was 2.1:1:9.1:0.025 which was nearly to ideal value within the allowable measurement uncertainties.

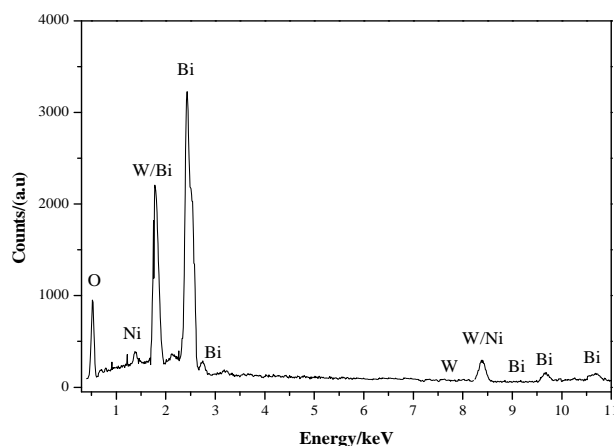


Fig. 2 EDS images of 3% Ni/Bi₂WO₆ powders

3.1.3 SEM images of Ni²⁺/Bi₂WO₆

Figure 3 showed the SEM images of the Bi₂WO₆ with 3% Ni²⁺. The particles of Bi₂WO₆ exhibited looseness of structure and the shapes like peony with the average diameter of 1~2μm (Fig.3a). When the dosage of Ni²⁺ increased to 1%, the particles of Bi₂WO₆ showed spherical shape like the nest which was composed of nanosheets with the same size (Fig.3b). The aggregation of microballoon spheres appeared when the dosage of Ni²⁺ increased to 3%. Thus the surface of the particles became looser and the appearance was much different (Fig.3c). But the structure like spherical shape was not obviously and the nanosheets disappeared after the dosage of Ni²⁺ increased to 5% (Fig.3d).

Based on the results we could see that the morphology of Bi₂WO₆ was influenced greatly by the Ni²⁺ doping. When the Ni²⁺ was 1%, the particles of Bi₂WO₆ could be prepared with nanostructure like peony. But with the increasing Ni²⁺, much more Ni²⁺ were absorbed on the surface of the particles causing porous channel plugging and lower catalytic activity.

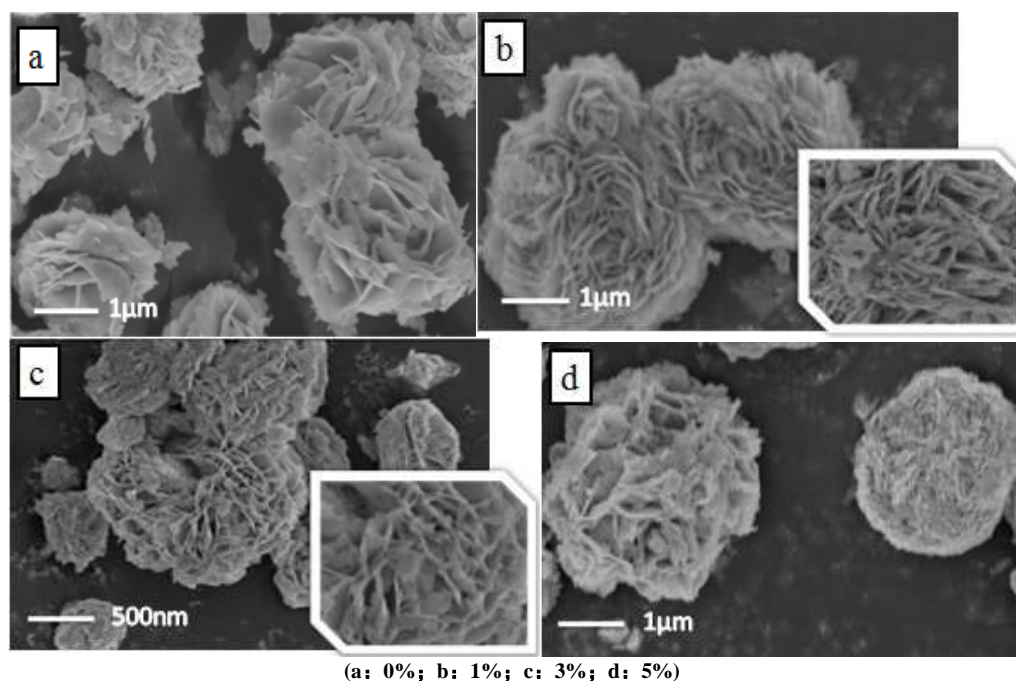


Fig. 3 SEM images of different Bi₂WO₆ powders

3.1.4 The specific surface area and pore size distributions of Ni²⁺/Bi₂WO₆

Figure 4 showed the pore size distributions and N₂ adsorption-desorption isotherm of Ni²⁺/Bi₂WO₆. The adsorption-desorption isotherm of the catalyst had a distinct hysteresis loop in the p/p₀ of 0.5–0.9 and belonged to the type IV isotherm in the IUPAC classification, which is characteristic of porous materials. It also could be found that the pore diameter was mainly about 4.5nm, the pore size distribution was narrow and the pore structure was

homogeneous being consistent with all of the information in the N₂ adsorption-desorption isotherm, that indicated the pore diameter and distributions were depended on the morphology of the catalyst.

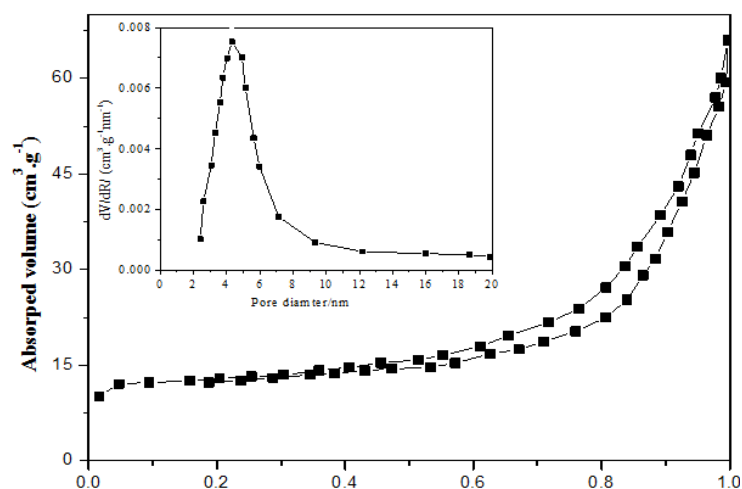


Fig. 4 N₂ gas adsorption-desorption isotherm of as-synthesized Bi₂WO₆ with 1% Ni²⁺

3.1.5 DR UV-vis spectroscopy of Ni²⁺/Bi₂WO₆

Figure 5 showed the UV-vis spectra of Bi₂WO₆ with different dosage of Ni²⁺. A red-shift occurred to the adsorption peak of Ni²⁺/Bi₂WO₆ compared with Bi₂WO₆. The absorption edges were 465nm and 482nm and the band gaps were 2.67eV and 2.57eV respectively that indicated doping Ni²⁺ could broaden the photoabsorption region of Bi₂WO₆ conforming the results from XRD and EDS. We could make sure further doping Ni²⁺ could influence the morphology and the particle size of the catalyst that caused more compact structure and strong coupling effect.¹² All of the above factors improved the activity of the catalyst.

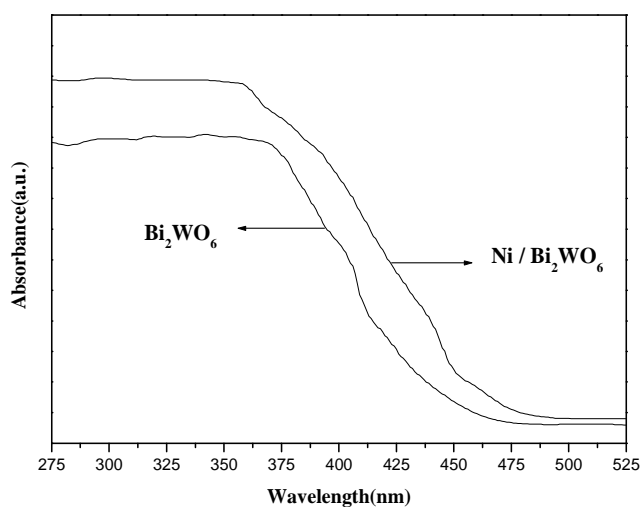


Fig. 5 UV-Vis diffuse reflectance spectra of Bi₂WO₆ with 1% Ni²⁺

3.1.6 The interaction between pyridine in the simulated oil and Ni²⁺/Bi₂WO₆

In order to research the interaction between pyridine in the simulated oil and the surface of Ni²⁺/Bi₂WO₆, the acid type on the surface of Ni²⁺/Bi₂WO₆ was measured by Py-FT-IR and the result was showed in Figure 7. It was clearly that two characteristic absorption peaks appeared after pyridine adsorbing on the surface of Ni²⁺/Bi₂WO₆, one was 1450 cm⁻¹ which was also the characteristic absorption peak of L-acid and the other was 1620 cm⁻¹ which was also the characteristic absorption peak of B-acid.^[13,14] The analysis indicated that the acid sites on the catalyst were mostly contributed by L-acid. So pyridine in the simulated oil reacted with the surface of Ni²⁺/Bi₂WO₆ through the lone pair electrons of Ni and chemical bond formed not only physical adsorption.

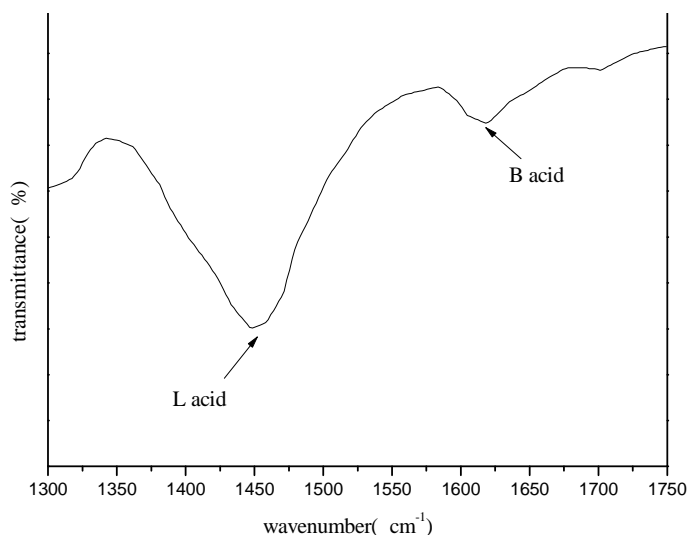


Fig. 6 $\text{Ni}^{2+}/\text{Bi}_2\text{WO}_6$ IR spectra of pyridine adsorption

3.2 Photocatalytic denitrification activity of $\text{Ni}^{2+}/\text{Bi}_2\text{WO}_6$

Figure 7 showed the effect of reaction time on the of simulated oil obtained with various Ni loading under the following conditions: catalysts to simulated oil ratio was 2 mg/40 ml, shined by a 500-W xenon lamp and nitrogen content in the simulated oil was 100 ppb. It was clear that the denitrogenation degree changed with the reaction time in the same patterns under different Ni loading. The denitrogenation activity after doping Ni was higher obviously than Bi_2WO_6 without Ni. When the reaction time was 120 min, the highest denitrogenation degree could be 94% at 1% loading on Bi_2WO_6 . The results indicated that doping Ni with proper dosage on Bi_2WO_6 could result in the form of trap capturing charge carrier and high recombination rate of photoelectron and electron hole, so the denitrogenation activity was improved at last.

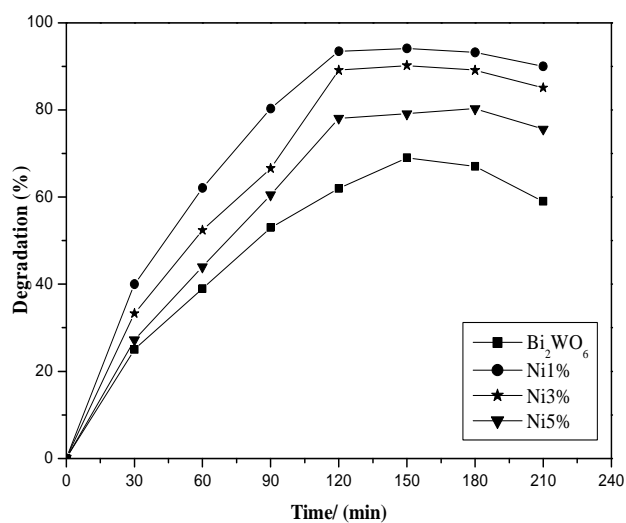


Fig. 7 The photocatalytic activity of Bi_2WO_6 with various Ni loading

CONCLUSION

The Ni-doped Bismuth tungstate (Bi_2WO_6) microcrystalline was successfully prepared by a facile hydrothermal route in the paper and the conclusions were as follows:

Doping Ni^{2+} properly on Bi_2WO_6 could lead to regular and compact structure, homogeneous pore diameter, larger special surface and lower photoabsorption region. All of the above indicated that the spectral absorption range extended to visible region and thus the photocatalytic denitrification activity was increased.

The rate of the $\text{Ni}/\text{Bi}_2\text{WO}_6$ powder could reach to 94% under the the following conditions that photocatalytic

reaction time was 120 min, Ni²⁺ doping content was 1%, ratio of catalyst to oil was 20 mg/40ml.

Acknowledgements

This work was supported by the Chinese National Natural Science Foundation (50476091), Hei Longjiang Programs for Science and Technology Development (11513009) and Education graduate science and technology innovation fund project in Heilongjiang province (YJSCX2001-135HLJ)

REFERENCES

- [1] CL Georgina; L. Sara, A. Regina, et al. *Fuel*, **2002**, 81: 1341-1350.
- [2] Y Sano; K H. Choi; Y Korai, et al. *Applied Catalysis B: Environmental*, **2004**, 53(3): 169-174.
- [3] H Huang; H Chen, Y Xia; et al. *Journal of colloid and interface science*, **2012**, 370(1): 132-138.
- [4] Y Yan; Y Wu; Y Yan; et al. *Journal of Physical Chemistry C*, **2013**, 117(39): 20017-20028.
- [5] Q Xiao; J Zhang; C Xiao, et al. *Catalysis Communications*, **2008**, 9(6): 1247-1253.
- [6] J He; W Wang; F Long; et al. *Materials Science and Engineering: B*, **2012**, 177(12): 967-974.
- [7] H Fu; W Yao; L Zhang; et al. *Materials Research Bulletin*, **2008**, 43(10): 2617-2625.
- [8] SH-T01629, Alkaline nitrogen determination method in petroleum products [S].
- [9] C Wang; H Zhang; F Li; et al. *Environmental science & technology*, **2010**, 4(17): 6843-6848.
- [10] Y Li; J Liu; X Huang; et al. *Crystal growth & design*, **2007**, 7(7): 1350-1355.
- [11] XH Zhang; LT Luo. *Jouranl of the Chinese ceramic society*, **2005**, 33(1): 12-16.
- [12] MS Gui; WD Zhang; Q X. Su; et al. *Journal of Solid State Chemistry*, **2011**, 184(8): 1977-1982.
- [13] D Dambournet; H Leclerc; A Vimont; et al. *Physical Chemistry Chemical Physics*, **2009**, 11(9): 1369-1379.
- [14] JM Song ; H Wang; YP Li . *Science China Press B*, **2013**(2):163-170.
- [15] WD Wang ; EC Yang JK Hao. *Chemical Journal of Chinese Universities*, **2002**, 12:2256-2260.
- [16] XB Wang ; K Zhao; DJ Kong. *Journal of engineering thermophysics*, **2008**, 07:1147-1150.